MJFAS MALAYSIAN JOURNAL OF FUNDAMENTAL AND APPLIED SCIENCES
PRINT ISSN: 2289-5981 | ONLINE ISSN: 2289-599X

RESEARCH ARTICLE

Darcy-Benard double diffusive Marangoni convection in a composite layer system with constant heat source along with non uniform temperature gradients

Manjunatha N [a,*], Sumithra R [b], Vanishree R K [c]

[a] Department of Mathematics, School of Applied Sciences, REVA University, Bengaluru, Karnataka, India
[b] Department of UG, PG Studies & Research in Mathematics, Government Science College Autonomous, Bengaluru, Karnataka, India
[c] Department of Mathematics, Maharani's Science College for Women, Maharani's Cluster University, Bengaluru, Karnataka, India

* Corresponding author: manjunatha.n@reva.edu.in

Article history
Received 21 July 2020
Revised 20 September 2020
Accepted 22 September 2020

Abstract

The problem of Benard double diffusive Marangoni convection is investigated in a horizontally infinite composite layer system enclosed by adiabatic boundaries for Darcy model. This composite layer is subjected to three temperature gradients with constant heat sources in both the layers. The lower boundary of the porous region is rigid and upper boundary of the fluid region is free with Marangoni effects. The Eigenvalue problem of a system of ordinary differential equations is solved in closed form for the Thermal Marangoni number, which happens to be the Eigen value. The three different temperature profiles considered are linear, parabolic and inverted parabolic profiles with the corresponding thermal Marangoni numbers are obtained. The impact of the porous parameter, modified internal Rayleigh number, solute Marangoni number, solute diffusivity ratio and the diffusivity ratio on Darcy-Benard double diffusive Marangoni convection are investigated in detail.

Keywords: Darcy model, Adiabatic boundaries, Depth ratio, Composite layer, Heat source and Three profiles.

INTRODUCTION

Double diffusive convection is a convection which is amalgamation of two density gradients diffusing at different rates, acting on a system. Double diffusion convection plays a significant role in many natural processes and has a lot of engineering applications. Double diffusive convection exists in sea water, the mantle flow in the Earth's crust as well as many engineering and physical problems. For example, contaminant transport in saturated soils, food processing, spread of toxins and furthermore appears in the modeling of solar ponds. The problems of double diffusive convection in single fluid /porous /composite layers / temperature gradients / heat source/sink are investigated by some authors. Bennacer et al. (2003) have analyzed numerically thermosolutal natural convection in an enclosure filled with fluid and two saturated porous layers. Chen and Cho Lik Chen (2010) have examined the stability of convection in a horizontal double-diffusive fluid layer driven by the combined effects of buoyancy and surface tension using linear stability analysis. Gangadharaiah and Suma (2013) considered Bernard-Marangoni convection in a fluid layer overlying a layer of an anisotropic porous layer with deformable free surface using regular perturbation technique. Double-diffusive convection in vertical annuluses with contradicting temperature and concentration gradients is of essential intrigue and viable significance examined by Sheng Chen et al. (2014) using lattice Boltzmann model. Saleem et al. (2014) investigated the double diffusive Marangoni convection flow of viscous incompressible electrically conducting fluid in a square cavity is studied using successive over relaxation technique. Sumithra (2014) studied the double diffusive magneto Marangoni convection in a composite layer using perturbation technique. Double-diffusive natural convection in vertical square enclosures induced by opposite horizontal temperature and concentration gradients is studied numerically by Massimo Corcione et al. (2015). Norazam Arbin et al. (2016) have studied the double diffusive Marangoni convection in the presence of entropy generation numerically using finite difference method. They showed that the heat and mass transfer have similar patterns as the Marangoni number increased. Akil J. Harfash., Fahad K. Nashmi (2017) studied the double-diffusive convection in the presence of heat sink/source which is linear in the vertical coordinate in the opposite direction to gravity by considering a horizontal fluid layer. The onset of double-diffusive convection in a superposed fluid and porous layer under high-frequency and small-amplitude vibrations has been experimented by Tatyana and Ekaterina (2018). Kanchana et al. (2020) studied the Kuppers-Lortz instability in rotating Rayleigh-Benard convection bounded by rigid/free isothermal boundaries. They show that alumina nanoparticles in water and alumina and copper in water have the same effect. For the composite layer, Sumithra et al. (2020) and Vanishree et al. (2020) are obtained the closed form solution for the eigenvalue problem in the presence of constant heat source.

In this article, the problem of Benard double diffusive Marangoni convection is investigated in a horizontally infinite composite layer system enclosed by adiabatic boundaries for the Darcy model. The Eigen value problem of a system of ordinary differential equations is solved in closed form for the thermal Marangoni number. The impact of different parameters is discussed in detail.

MATHEMATICAL FORMULATION

The composite layer system under investigation is shown in Fig. 1. A horizontal densely packed porous layer of thickness d_m underlying a

two component fluid layer of thickness d with heat constant sources Q_m and Q respectively. The lower surface of the porous layer rigid and the upper surface of the fluid layer is free with surface tension effects depending on both temperature and concentration. Both the boundaries are kept at different constant temperatures and salinities. We introduce Cartesian co-ordinate system at the interface between porous and fluid layer and the z-axis directing vertically upwards.

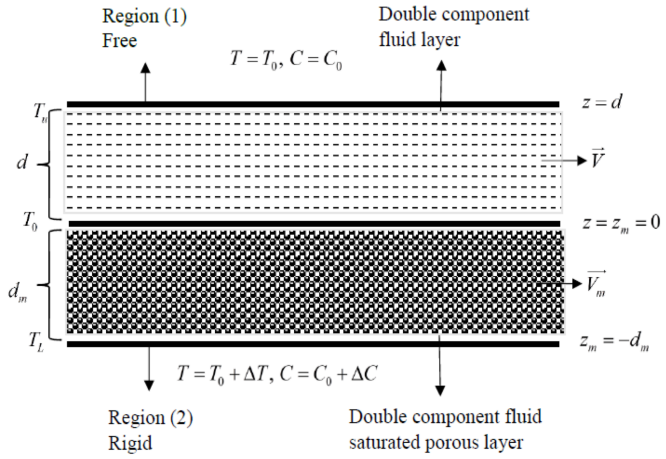

Figure 1. Physical configuration of problem.

The governing equations for the physical situation considered under microgravity condition:

Fluid layer:

$$\nabla.\vec{V} = 0 \tag{1}$$

$$\rho_0[\frac{\partial \vec{V}}{\partial t} + (\vec{q}.\nabla)\vec{V}] = -\nabla P + \mu\nabla^2\vec{V} \tag{2}$$

$$\frac{\partial T}{\partial t} + (\vec{V}.\nabla)T = \kappa\nabla^2 T + Q \tag{3}$$

$$\frac{\partial C}{\partial t} + (\vec{V}.\nabla)C = \kappa_c\nabla^2 C \tag{4}$$

Porous layer:

$$\nabla_m.\overrightarrow{V_m} = 0 \tag{5}$$

$$\rho_0[\frac{1}{\phi}\frac{\partial \overrightarrow{V_m}}{\partial t} + \frac{1}{\phi^2}(\overrightarrow{V_m}.\nabla_m)\overrightarrow{V_m}] = -\nabla_m P_m - \frac{\mu}{K}\overrightarrow{V_m} \tag{6}$$

$$A\frac{\partial T_m}{\partial t} + (\overrightarrow{V_m}.\nabla_m)T_m = \kappa_m\nabla_m^2 T_m + Q_m \tag{7}$$

$$\phi\frac{\partial C_m}{\partial t} + (\overrightarrow{V_m}.\nabla_m)C_m = \kappa_{cm}\nabla_m^2 C_m \tag{8}$$

Here, $\vec{V}$, ρ_0, μ, P, T, κ, κ_c, C, K, A, ϕ are referring to the velocity vector, the fluid density, the fluid viscosity, the pressure, the temperature, the thermal diffusivity of the fluid, the solute diffusivity of the fluid, the concentration, the permeability of the porous medium, the ratio of heat capacities and the porosity, respectively, and the subscript 'm' refer to the quantities in porous layer.

The basic state is quiescent, have the following solutions

Fluid layer:

$$\vec{V} = 0,\ P = P_b(z),\ T = T_b(z),\ C = C_b(z) \tag{9}$$

Porous layer:

$$\overrightarrow{V_m} = 0, P_m = P_{mb}(z_m), T_m = T_{mb}(z_m), C_m = C_{mb}(z_m) \tag{10}$$

The temperature distribution in the basic state are obtained by

$$T_b(z) = \frac{-Qz(z-d)}{2\kappa} + \frac{(T_u - T_0)f(z)}{d} + T_0 \quad 0 \le z \le d \tag{11}$$

$$\left.\begin{aligned} T_{mb}(z_m) = \frac{-Q_m z_m(z_m + d_m)}{2\kappa_m} + \frac{(T_0 - T_l)f_m(z_m)}{d_m} + T_0 \\ -d_m \le z_m \le 0 \end{aligned}\right\} \tag{12}$$

The concentration distributions in the basic state are obtained by

$$C_b(z) = C_0 - \frac{(C_0 - C_u)z}{d} \qquad 0 \le z \le d \tag{13}$$

$$C_{mb}(z_m) = C_0 - \frac{(C_l - C_0)z_m}{d_m} \qquad -d_m \le z_m \le 0 \tag{14}$$

where

$T_0 = \frac{\kappa d_m T_u + \kappa_m d T_l}{\kappa d_m + \kappa_m d} + \frac{d d_m(Q_m d_m + Qd)}{2(\kappa d_m + \kappa_m d)}$ is the interface temperature,

$C_0 = \frac{\kappa_c d_m C_u + \kappa_{cm} d C_l}{\kappa_c d_m + \kappa_{cm} d}$ is the interface concentration,

$f(z)$ & $f_m(z_m)$ are the temperature gradients in fluid & porous layer

with $\int_0^1 f(z)dz = 1$ and $\int_0^1 f_m(z_m)\,dz_m = 1$, respectively.

To investigate the stability of the basic state, infinitesimal disturbances are superimposed on fluid and porous layer, respectively.

$$\vec{V} = \vec{V}', P = P_b + P',\ T = T_b(z) + \theta, C = C_b(z) + S \tag{15}$$

$$\left.\begin{aligned} \overrightarrow{V_m} = \overrightarrow{V_m}', P_m = P_{mb} + P_{m'}, T_m = T_{mb}(z_m) + \theta_m, \\ C_m = C_{mb}(z_m) + S_m \end{aligned}\right\} \tag{16}$$

Following the standard linear stability analysis procedure and noting that the principle of exchange of stability holds (Sumithra et al.,2020), we arrive at the following stability equations:

$$(D^2 - a^2)^2 W(z) = 0 \tag{17}$$

$$(D^2 - a^2)\theta(z) + [f(z) + R_I^*(2z-1)]W(z) = 0 \tag{18}$$

$$\tau(D^2 - a^2)S(z) + W(z) = 0 \tag{19}$$

$$(D_m^2 - a_m^2)W_m(z_m) = 0 \tag{20}$$

$$(D_m^2 - a_m^2)\theta_m(z_m) + [f_m(z_m) + R_{Im}^*(2z_m + 1)]W_m(z_m) = 0 \tag{21}$$

$$\tau_{pm}(D_m^2 - a_m^2)S_m(z_m) + W_m(z_m) = 0 \tag{22}$$

Here, $R_I^* = \frac{R_i}{2(T_0 - T_u)}$, $R_i = \frac{Qd^2}{\kappa}$, $\tau = \frac{\kappa_c}{\kappa}$ are known as the modified internal Rayleigh number, the internal Rayleigh number, the diffusivity ratios for fluid layer, respectively, and $R_{Im}^* = \frac{R_{im}}{2(T_l - T_0)}$, $R_{im} = \frac{Q_m d_m^2}{\kappa_m}$, $\tau_{pm} = \frac{\kappa_{cm}}{\kappa_m}$ are referring to the modified internal Rayleigh number, the internal Rayleigh number, and the diffusivity ratio for porous layer, respectively. $W(z)$ & $W_m(z_m)$ are the vertical velocities, $\theta(z)$ & $\theta_m(z_m)$ are the temperature distributions and $S(z)$ & $S_m(z_m)$ are the concentration distributions in fluid and porous layers, respectively. a and a_m are the horizontal wave numbers. Since the horizontal wave numbers must be the same for the composite layers, so that we have $\frac{a}{d} = \frac{a_m}{d_m}$ and hence $a_m = \hat{d}a$. where $\hat{d} = \frac{d_m}{d}$ is the depth ratio.

BOUNDARY CONDITIONS

The following boundary conditions are used to solve the equations (17) to (22) and they are

$$D^2W(1) + Ma^2\theta(1) + M_s a^2 S(1) = 0 \tag{23}$$

The velocity boundary conditions are

$$\begin{aligned} &W(1) = 0, W_m(-1) = 0, D_m W_m(-1) = 0, \hat{T}W(0) = W_m(0), \\ &\hat{T}d^2(D^2 + a^2)W(0) = \hat{\mu}(D_m^2 + a_m^2)W_m(0), \\ &\hat{T}d^3\beta^2(D^3W(0) - 3a^2DW(0)) = -D_m W_m(0) \end{aligned} \tag{24}$$

The temperature distribution boundary conditions are

$$D\theta(1) = 0, \theta(0) = \hat{T}\theta_m(0), D\theta(0) = D_m\theta_m(0), D_m\theta_m(-1) = 0 \tag{25}$$

The salinity distribution boundary conditions are

$$DS(1) = 0, S(0) = \hat{S}S_m(0), DS(0) = D_m S_m(0), D_m S_m(-1) = 0 \tag{26}$$

where

$\hat{S} = \frac{C_l - C_0}{C_0 - C_u}$, $\hat{T} = \frac{T_l - T_0}{T_0 - T_u}$, $\hat{\mu} = \frac{\mu_m}{\mu}$, μ_m, $M = -\frac{\partial\sigma_t}{\partial T}\frac{(T_0 - T_u)d}{\mu\kappa}$, $M_s = -\frac{\partial\sigma_t}{\partial C}\frac{(C_0 - C_u)d}{\mu\kappa}$, σ_t, $\beta^2 = \frac{K}{d_m^2} = Da$ and β are respectively the solute diffusivity ratio, the thermal ratio, the viscosity ratio, the effective viscosity of the fluid in the porous layer, the thermal Marangoni number, the solute Marangoni number, the surface tension, the Darcy number, and the porous parameter.

SOLUTION BY EXACT TECHNIQUE

The solutions of $W(z)$ and $W_m(z_m)$ are obtained from equations (17) and (20), as follows

$$W(z) = A_1[\cosh az + a_1 z\cosh az + a_2\sinh az + a_3 z\sinh az] \tag{27}$$

$$W_m(z_m) = A_1[a_4\cosh a_m z_m + a_5\sinh a_m z_m] \tag{28}$$

where $a_1 - a_5$ are determined using (24) we get,

$$a_1 = \frac{a_m\coth a_m}{2a^3\beta^2 d^3}, a_2 = -1 - (a_1 + a_3)\tanh a,$$

$$a_3 = \frac{a_m^2\hat{\mu} - a^2d^2}{ad^2}, a_4 = \hat{T}, a_5 = \hat{T}\coth a_m$$

Linear temperature profile

The linear temperature profile of the form,

$$f(z) = 1 \quad \& \quad f_m(z_m) = 1 \tag{29}$$

introducing (29) in to (18) and (21), we get the $\theta(z)$ and $\theta_m(z_m)$ as follows

$$\theta(z) = A_1[c_1\cosh az + c_2\sinh az + g_1(z)] \tag{30}$$

$$\theta_m(z_m) = A_1[c_3\cosh a_m z_m + c_4\sinh a_m z_m + g_{1m}(z_m)] \tag{31}$$

where $c_1 - c_4$ are determined using (25) we get,

$$g_1(z) = A_1[\Delta_1 - \Delta_2 + \Delta_3 - \Delta_4], g_{1m}(z_m) = A_1[\Delta_5 - \Delta_6]$$

$$\Delta_1 = \frac{(2E_1 z + E_2 z^2)}{4a}(a_1\cosh az + \sinh az)$$

$$\Delta_2 = \frac{E_2 z}{4a^2}(\cosh az + a_1\sinh az)$$

$$\Delta_3 = \frac{(6a^2z^2E_1 + 4a^2z^3E_2 + 6E_2 z)}{24a^3}(a_3\cosh az + a_2\sinh az)$$

$$\Delta_4 = \frac{(E_1 z + E_2 z^2)}{4a^2}(a_2\cosh az + a_3\sinh az)$$

$$\Delta_5 = \frac{(2E_{1m}z_m + E_{2m}z_m^2)}{4a_m}(a_5\cosh a_m z_m + a_4\sinh a_m z_m)$$

$$\Delta_6 = \frac{E_{2m}z_m}{4a_m^2}(a_4\cosh a_m z_m + a_5\sinh a_m z_m)$$

$$E_1 = R_I^* - 1, E_2 = -2R_I^*, E_{1m} = -(R_{Im}^* + 1), E_{2m} = -2R_{Im}^*,$$

$$c_1 = c_3\hat{T}, c_2 = \frac{1}{a}(c_4 a_m + \delta_3 - \delta_2), c_3 = \frac{\delta_8}{\delta_9}, c_4 = \frac{\delta_6}{\delta_7},$$

$$\delta_1 = -A_1[\Delta_7 + \Delta_8 + \Delta_9 + \Delta_{10}]$$

$$\Delta_7 = \frac{(2a^2E_1 + E_2(a^2 - 1))}{4a^2}(\cosh a + a_1\sinh a)$$

$$\Delta_8 = \frac{E_2 + 2E_1}{4a}(a_1\cosh a + \sinh a)$$

$$\Delta_9 = \frac{(3a^2 - 3)E_1 + (2a^2 - 3)E_2}{12a^2}(a_2\cosh a + a_3\sinh a)$$

$$\Delta_{10} = \frac{(a^2E_1 + E_2(a^2 + 1))}{4a^3}(a_3\cosh a + a_2\sinh a)$$

$$\delta_2 = A_1\left[\frac{(2a^2a_1 - aa_2)E_1 + (a_3 - a)E_2}{4a^3}\right]$$

$$\delta_3 = A_1[\frac{2E_{1m}a_5}{4a_m} - \frac{a_4E_{2m}}{4a_m^2}], \ \delta_4 = -A_1[\Delta_{11} + \Delta_{12}]$$

$$\Delta_{11}=[\frac{E_{2m}-2E_{1m}}{4}-\frac{E_{2m}}{4a_m^2}](a_4\cosh a_m-a_5\sinh a_m)$$

$$\Delta_{12}=[\frac{2E_{1m}-E_{2m}}{4a_m}](a_5\cosh a_m-a_4\sinh a_m),$$

$$\delta_5=\delta_1-(\delta_3-\delta_2)\cosh a$$

$$\delta_6=\delta_4 a\hat{T}\sinh a+\delta_5 a_m\sinh a_m$$

$$\delta_7=a_m\cosh a_m a\hat{T}\sinh a+a_m^2\cosh a\sinh a_m$$

$$\delta_8=\delta_4\cosh a-\delta_5\cosh a_m$$

$$\delta_9=-a\cosh a_m\hat{T}\sinh a-a_m\cosh a\sinh a_m$$

From (19) and (22), we get $S(z)$ and $S_m(z_m)$ as,

$$S(z)=A_1[c_{13}\cosh az+c_{14}\sinh az+g(z)] \tag{32}$$

$$S_m(z_m)=A_1[c_{15}\cosh a_m z_m+c_{16}\sinh a_m z_m+g_m(z_m)] \tag{33}$$

where $c_{13}-c_{16}$ are determined using (26) we get,

$$g(z)=\frac{-1}{\tau}[(\frac{a_1 z}{2a}+\frac{a_3 z^2}{4a}-\frac{a_2 z}{4a^2})\cosh az+(\frac{z}{2a}+\frac{a_2 z^2}{4a}-\frac{a_3 z}{4a^2})\sinh az]$$

$$g_m(z_m)=-\frac{z_m}{2a_m\tau_{pm}}[(a_5\cosh a_m z_m+a_4\sinh a_m z_m)]$$

$$c_{13}=\hat{S}c_{15}, c_{14}=\frac{1}{a}(c_{16}a_m+\Delta_{101}-\Delta_{102}),$$

$$c_{15}=\frac{\Delta_{106}a_m\cosh a_m-\Delta_{103}\Delta_{105}}{\Delta_{105}a_m\sinh a_m+\Delta_{104}a_m\cosh a_m},$$

$$c_{16}=\frac{\Delta_{103}\Delta_{104}+\Delta_{106}a_m\sinh a_m}{\Delta_{105}a_m\sinh a_m+\Delta_{104}a_m\cosh a_m},$$

$$\Delta_{100}=\frac{1}{\tau}[\frac{1}{2}(\cosh a+a_1\sinh a)+\frac{1}{2a}(a_1\cosh a+\sinh a)+\Delta_{1000}],$$

$$\Delta_{1000}=\frac{(a^2-1)}{4a^2}(a_2\cosh a+a_3\sinh a)+\frac{1}{4a}(a_3\cosh a+a_2\sinh a),$$

$$\Delta_{101}=-\frac{a_5}{2a_m\tau_{pm}}, \Delta_{102}=-\frac{1}{\tau}(\frac{a_1}{2a}-\frac{a_2}{4a^2}),$$

$$\Delta_{103}=-\frac{1}{2\tau_{pm}}(a_4\cosh a_m-a_5\sinh a_m)$$
$$+\frac{1}{2a_m\tau_{pm}}(a_5\cosh a_m-a_4\sinh a_m),$$

$$\Delta_{104}=\hat{S}a\sinh a, \Delta_{105}=a_m\cosh a,$$

$$\Delta_{106}=\Delta_{100}-(\Delta_{101}-\Delta_{102})\cosh a$$

Using (23), for the linear temperature profile we get the thermal Marangoni number as follows

$$M_1=\frac{-\Lambda_1}{a^2(c_1\cosh a+c_2\sinh a+\Lambda_2+\Lambda_3)} \tag{34}$$

where

$$\Lambda_1=\Delta_{13}+\Delta_{14},$$

$$\Delta_{13}=a^2(\cosh a+a_1\sinh a)+a_2(a^2\cosh a+2a\sinh a)$$

$$\Delta_{14}=a_3(a^2\sinh a+2a\cosh a)$$

$$\Lambda_2=(\frac{E_2+2E_1}{4a})R_1-\frac{E_2}{4a^2}R_2$$

$$R_1=(a_1\cosh a+\sinh a),$$

$$R_2=(\cosh a+a_1\sinh a),\quad \Lambda_3=\Delta_{15}-\Delta_{16},$$

$$\Delta_{15}=\frac{(4a^2E_2+6a^2E_1+6E_2)}{24a^3}(a_3\cosh a+a_2\sinh a),$$

$$\Delta_{16}=\frac{(E_2+E_1)}{4a^2}(a_3\sinh a+a_2\cosh a)$$

Parabolic temperature profile

The parabolic temperature profile of the form,

$$f(z)=2z \quad \& \quad f_m(z_m)=2z_m \tag{35}$$

introducing (35) in to (18) and (21), we get the $\theta(z)$ and $\theta_m(z_m)$ as follows

$$\theta(z)=A_1[c_5\cosh az+c_6\sinh az+g_2(z)] \tag{36}$$

$$\theta_m(z_m)=A_1[c_7\cosh a_m z_m+c_8\sinh a_m z_m+g_{2m}(z_m)] \tag{37}$$

where c_5-c_8 are determined (25) we get,

$g_2(z)=A_1[\Delta_{17}-\Delta_{18}+\Delta_{19}-\Delta_{20}]$, $g_{2m}(z_m)=A_1[\Delta_{21}-\Delta_{22}]$

$$\Delta_{17}=\frac{(2E_3z+E_4z^2)}{4a}(a_1\cosh az+\sinh az)$$

$$\Delta_{18}=\frac{E_4 z}{4a^2}(\cosh az+a_1\sinh az)$$

$$\Delta_{19}=\frac{(6a^2z^2E_3+4a^2z^3E_4+6E_4z)}{24a^3}(a_3\cosh az+a_2\sinh az)$$

$$\Delta_{20}=\frac{(E_3z+E_4z^2)}{4a^2}(a_2\cosh az+a_3\sinh az)$$

$$\Delta_{21}=\frac{(2E_{3m}z_m+E_{4m}z_m^2)}{4a_m}(a_5\cosh a_m z_m+a_4\sinh a_m z_m)$$

$$\Delta_{22}=\frac{E_{4m}z_m}{4a_m^2}(a_4\cosh a_m z_m+a_5\sinh a_m z_m)$$

$$E_3=R_I^*, E_4=-2(R_I^*+1), E_{3m}=-R_{Im}^*, E_{4m}=-2(R_{Im}^*+1),$$

$$c_5=c_7\hat{T}, c_6=\frac{1}{a}(c_8a_m+\delta_{12}-\delta_{11}),$$

$$c_7=\frac{\delta_{17}}{\delta_{18}}, c_8=\frac{\delta_{15}}{\delta_{16}}, \delta_{10}=-A_1[\Delta_{23}+\Delta_{24}+\Delta_{25}+\Delta_{26}]$$

$$\Delta_{23}=\frac{(2a^2E_3+E_4(a^2-1))}{4a^2}(\cosh a+a_1\sinh a)$$

$$\Delta_{24}=\frac{E_4+2E_3}{4a}(a_1\cosh a+\sinh a)$$

$$\Delta_{25}=\frac{(3a^2-3)E_3+(2a^2-3)E_4}{12a^2}(a_2\cosh a+a_3\sinh a)$$

$$\Delta_{26}=\frac{(a^2E_3+E_4(a^2+1))}{4a^3}(a_3\cosh a+a_2\sinh a),$$

$$\delta_{11}=A_1[\frac{(2a^2a_1-aa_2)E_3+(a_3-a)E_4}{4a^3}]$$

$$\delta_{12}=A_1[\frac{2E_{3m}a_5}{4a_m}-\frac{a_4E_{4m}}{4a_m^2}]\ \delta_{13}=-A_1[\Delta_{27}+\Delta_{28}],$$

$$\Delta_{27}=[\frac{E_{4m}-2E_{3m}}{4}-\frac{E_{4m}}{4a_m^2}](a_4\cosh a_m-a_5\sinh a_m)$$

$$\Delta_{28}=[\frac{2E_{3m}-E_{4m}}{4a_m}](a_5\cosh a_m-a_4\sinh a_m)$$

$\delta_{14} = \delta_{10} - (\delta_{12} - \delta_{11})\cosh a,$

$\delta_{15} = \delta_{13} a\hat{T}\sinh a + \delta_{14} a_m \sinh a_m$

$\delta_{16} = a_m \cosh a_m a\hat{T}\sinh a + a_m^2 \cosh a \sinh a_m,$

$\delta_{17} = \delta_{13}\cosh a - \delta_{14}\cosh a_m$

$\delta_{18} = -a\cosh a_m \hat{T}\sinh a - a_m \cosh a \sinh a_m$

Using (23), for the parabolic temperature profile we get the thermal Marangoni number as follows

$$M_2 = \frac{-\Lambda_1}{a^2(c_5\cosh a + c_6 \sinh a + \Lambda_4 + \Lambda_5)} \tag{38}$$

where

$\Lambda_4 = (\frac{(E_4 + 2E_3)}{4a})R_1 - \frac{E_4}{4a^2}R_2,\ \Lambda_5 = \Delta_{29} - \Delta_{30},$

$\Delta_{29} = \frac{(4a^2E_4 + 6a^2E_3 + 6E_4)}{24a^3}(a_3\cosh a + a_2 \sinh a),$

$\Delta_{30} = \frac{(E_4 + E_3)}{4a^2}(a_3 \sinh a + a_2 \cosh a)$

Inverted Parabolic Temperature Profile

The inverted parabolic temperature profile of the form,

$$f(z) = 2(1-z) \quad and \quad f_m(z_m) = 2(1-z_m) \tag{39}$$

introducing (39) in to (18) and (21), we get the $\theta(z)$ and $\theta_m(z_m)$ as follows

$$\theta(z) = A_1[c_9\cosh az + c_{10}\sinh az + g_3(z)] \tag{40}$$

$$\theta_m(z_m) = A_1[c_{11}\cosh a_m z_m + c_{12}\sinh a_m z_m + g_{3m}(z_m)] \tag{41}$$

where $c_9 - c_{12}$ are determined using (25) we get,

$g_3(z) = A_1[\Delta_{31} - \Delta_{32} + \Delta_{33} - \Delta_{34}],\ g_{3m}(z_m) = A_1[\Delta_{35} - \Delta_{36}]$

$\Delta_{31} = \frac{(2E_5 z + E_6 z^2)}{4a}(a_1\cosh az + \sinh az)$

$\Delta_{32} = \frac{E_6 z}{4a^2}(\cosh az + a_1 \sinh az)$

$\Delta_{33} = \frac{(6a^2z^2E_5 + 4a^2z^3E_6 + 6E_6 z)}{24a^3}(a_3\cosh az + a_2\sinh az)$

$\Delta_{34} = \frac{(E_5 z + E_6 z^2)}{4a^2}(a_2\cosh az + a_3\sinh az)$

$\Delta_{35} = \frac{(2E_{5m}z_m + E_{6m}z_m^2)}{4a_m}(a_5\cosh a_m z_m + a_4\sinh a_m z_m)$

$\Delta_{36} = \frac{E_{6m}z_m}{4a_m^2}(a_4\cosh a_m z_m + a_5\sinh a_m z_m)$

$E_5 = R_I^* - 2, E_6 = 2(1-R_I^*), E_{5m} = -2 - R_{Im}^*, E_{6m} = 2(1-R_{Im}^*)$

$c_9 = c_{11}\hat{T}, c_{10} = \frac{1}{a}(c_{12}a_m + \delta_{22} - \delta_{21})\ c_{11} = \frac{\delta_{26}}{\delta_{27}}, c_{12} = \frac{\delta_{24}}{\delta_{25}}$

$\delta_{19} = -A_1[\Delta_{37} + \Delta_{38} + \Delta_{39} + \Delta_{40}]$

$\Delta_{37} = \frac{(2a^2E_5 + E_6(a^2-1))}{4a^2}(\cosh a + a_1\sinh a)$

$\Delta_{38} = \frac{E_6 + 2E_5}{4a}(a_1\cosh a + \sinh a)$

$\Delta_{39} = \frac{(3a^2-3)E_5 + (2a^2-3)E_6}{12a^2}(a_2\cosh a + a_3\sinh a)$

$\Delta_{40} = \frac{(a^2E_5 + E_6(a^2+1))}{4a^3}(a_3\cosh a + a_2\sinh a)$

$\delta_{20} = -A_1[\Delta_{41} + \Delta_{42}],$

$\Delta_{41} = [\frac{E_{6m} - 2E_{5m}}{4} - \frac{E_{6m}}{4a_m^2}](a_4\cosh a_m - a_5\sinh a_m)$

$\Delta_{42} = [\frac{2E_{5m} - E_{6m}}{4a_m}](a_5\cosh a_m - a_4\sinh a_m)$

$\delta_{21} = A_1[\frac{(2a^2a_1 - aa_2)E_5 + (a_3 - a)E_6}{4a^3}]\ \delta_{22} = A_1[\frac{2E_{5m}a_5}{4a_m} - \frac{a_4E_{6m}}{4a_m^2}]$

$\delta_{23} = \delta_{19} - (\delta_{22} - \delta_{21})\cosh a,$

$\delta_{24} = \delta_{20} a\hat{T}\sinh a + \delta_{23} a_m \sinh a_m$

$\delta_{25} = a_m\cosh a_m a\hat{T}\sinh a + a_m^2\cosh a\sinh a_m$

$\delta_{26} = \delta_{20}\cosh a - \delta_{23}\cosh a_m$

$\delta_{27} = -a\cosh a_m\hat{T}\sinh a - a_m\cosh a\sinh a_m$

Using (23), for the inverted parabolic temperature profile we get the thermal Marangoni number as follows

$$M_3 = \frac{-\Lambda_1}{a^2(c_9\cosh a + c_{10}\sinh a + \Lambda_6 + \Lambda_7)} \tag{42}$$

where

$\Lambda_6 = (\frac{(E_6 + 2E_5)}{4a})R_1 - \frac{E_6}{4a^2}R_2$

$\Lambda_7 = \Delta_{43} - \Delta_{44}$

$\Delta_{43} = \frac{(4a^2E_6 + 6a^2E_5 + 6E_6)}{24a^3}(a_3\cosh a + a_2\sinh a)$

$\Delta_{44} = \frac{(E_6 + E_5)}{4a^2}(a_3\sinh a + a_2\cosh a)$

RESULTS AND DISCUSSION

Double diffusive Marangoni convection, produced by unstable density distribution with the surface tension effect, in a two-layer system is studied in the presence of constant heat source/sink. The Mathematica software is used to perform numerical calculations and to draw the graphs. The fluids are immiscible so that surface tension plays an important role. The effect of thermal Marangoni number versus the depth ratio $\hat{d}$, of the fluid layer for different parameters are drawn. The three different temperature profiles considered are linear, parabolic and inverted parabolic profiles with the corresponding thermal Marangoni numbers are M_1, M_2 and M_3. Figures 2 to 7 depict the effect of $\beta, R_{Im}^*, M_s, \hat{S}, \tau$ and τ_{pm} on M_1, M_2 and M_3 respectively for fixed values of $a = 1, M_s = 1, \hat{S} = \hat{T} = 1, \tau = \tau_{pm} = 1, R_I^* = R_{Im}^* = 1$ and $\beta = 0.1$.

Fig. 2(a, b, c) are the plots of M_1, M_2, and M_3 versus $\hat{d}$, for different values of the porous parameter β. From these figures, it is clear that the effect of β is to stabilize the system. Physically this implies that the increase in permeability gives extra space for the fluid movement thereby delaying the convection. It can be seen that M_1, M_2, and M_3 increase with $\hat{d}$ for all the three temperature profiles. One more observation that can be drawn from these figures is that the increase in depth ratio $\hat{d}$, indicating the dominance of the porous layer, beyond the equal depths of both the layers, increase M more rapidly. Moreover, one can observe that greater stability can be achieved by considering the inverted parabolic profile when the porous layer is dominant over the fluid layer.

The effect of modified internal Rayleigh number R_{Im}^{*} on thermal Marangoni numbers is seen in the Fig. 3(a, b, c), for the three temperature profiles. These figures indicate the stabilizing nature of R_{Im}^{*} (i.e., as R_{Im}^{*} increases, M_1, M_2 and M_3 increases). This delays the onset of convection. Physically increase in R_{Im}^{*} implies the increase in the strength of heat source. This increases the thermal Marangoni number. This effect is observed irrespective of the temperature profiles.

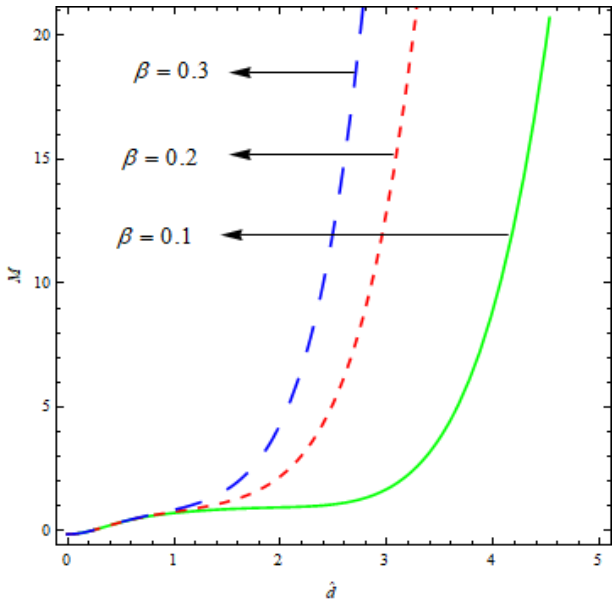

(a)

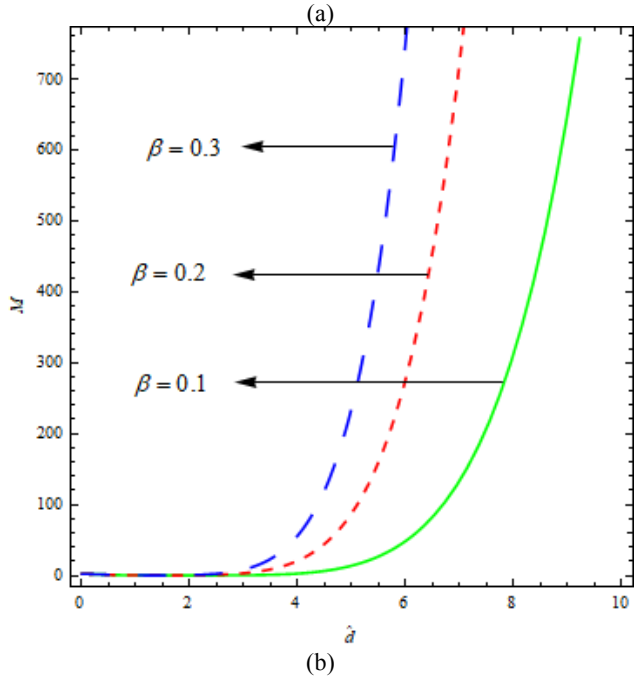

(b)

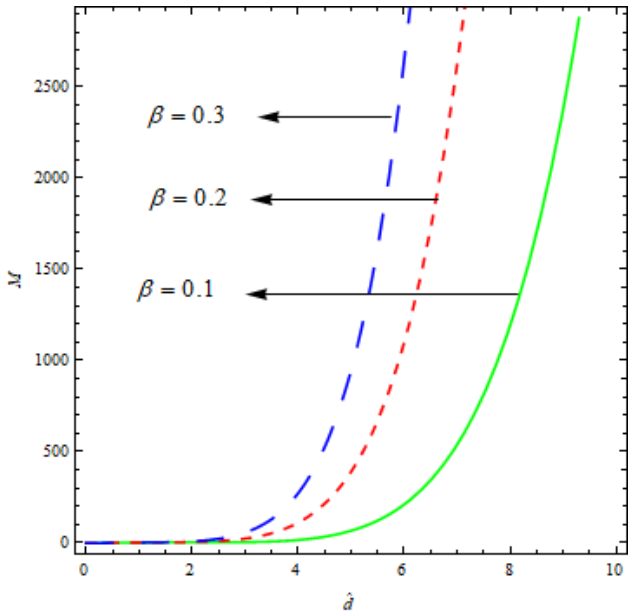

(c)

Fig. 2 M Versus $\hat{d}$ for different values of β

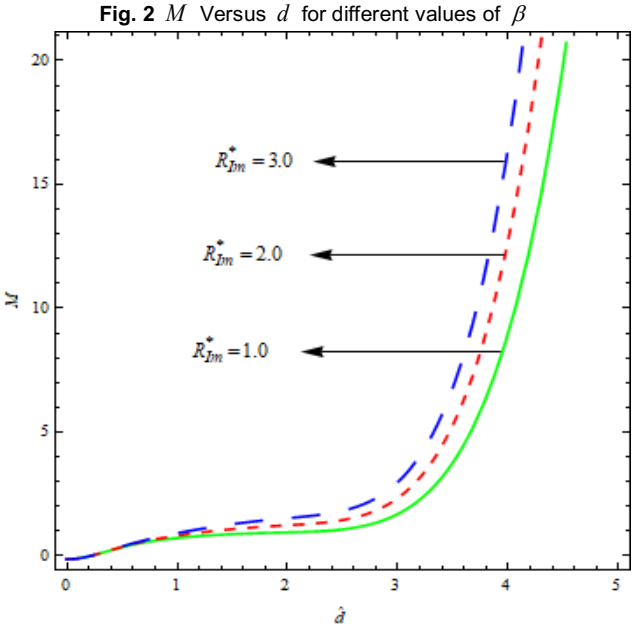

(a)

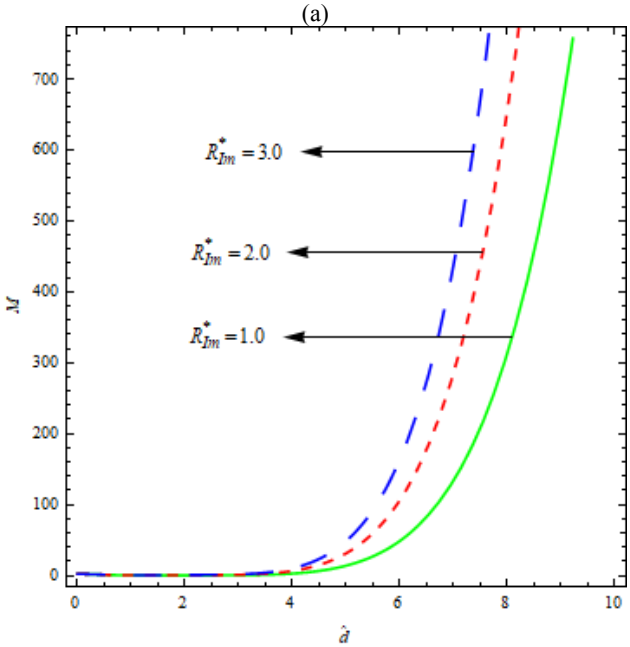

(b)

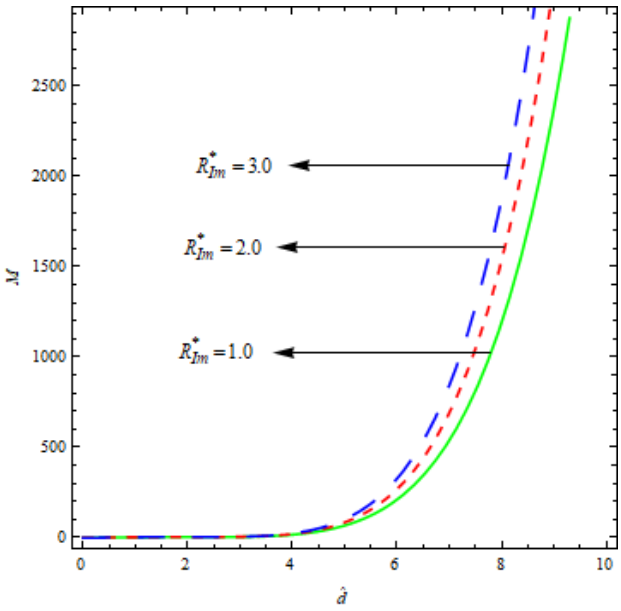

(c)

Fig. 3 M Versus $\hat{d}$ for different values of R^*_{Im}

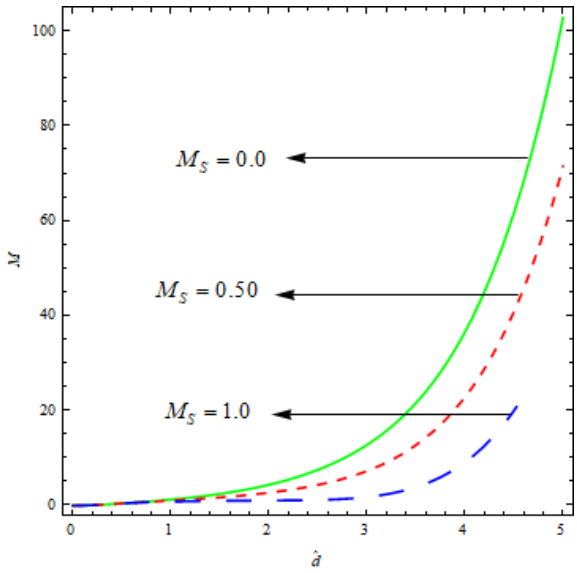

(a)

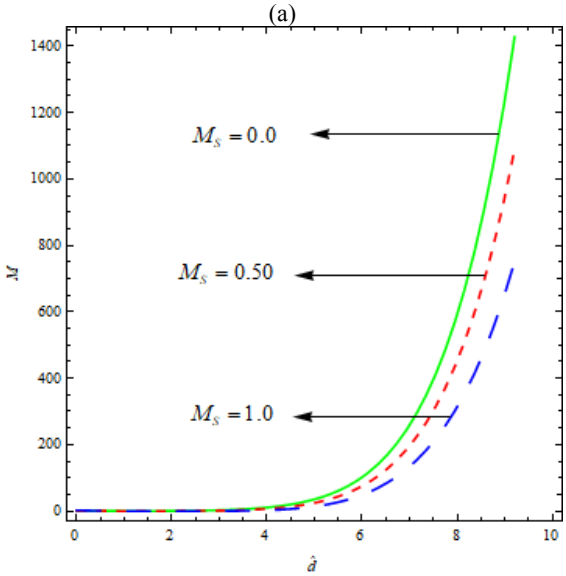

(b)

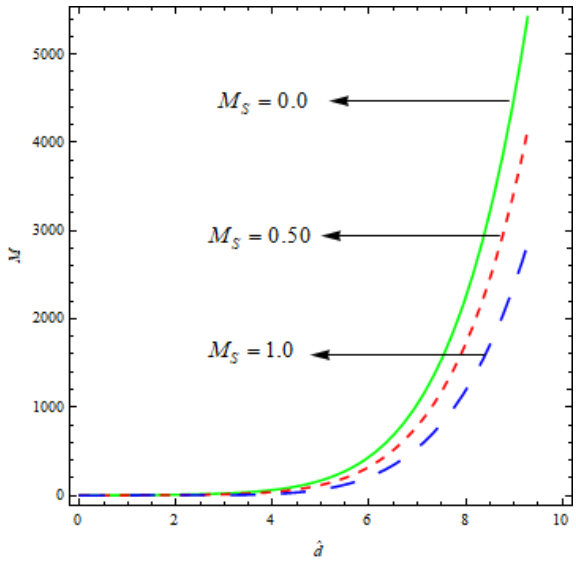

(c)

Fig. 4 M Versus $\hat{d}$ for different values of M_s

The plots of thermal Marangoni numbers M_1, M_2 and M_3 for different solute Marangoni number M_s are displayed in Fig. 4(a, b, c). The thermal Marangoni numbers M_1, M_2 and M_3 decreases with increase in M_s for linear, parabolic and inverted parabolic profiles. This helps in fastening convection. Thus, the system is destabilized. We see that the liquid convective movement is more predominant in the porous region.

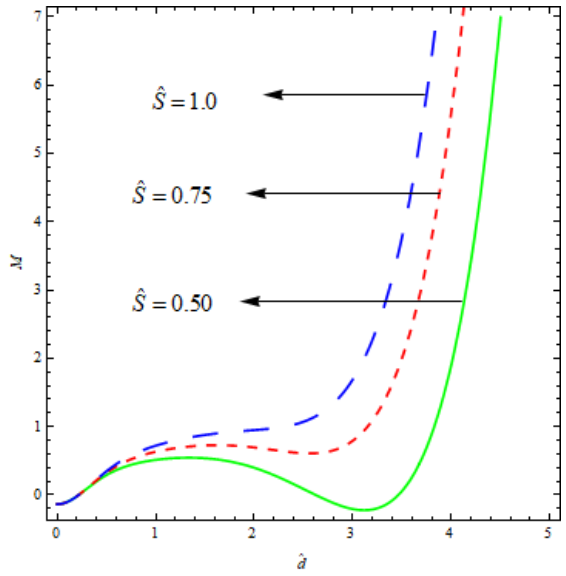

(a)

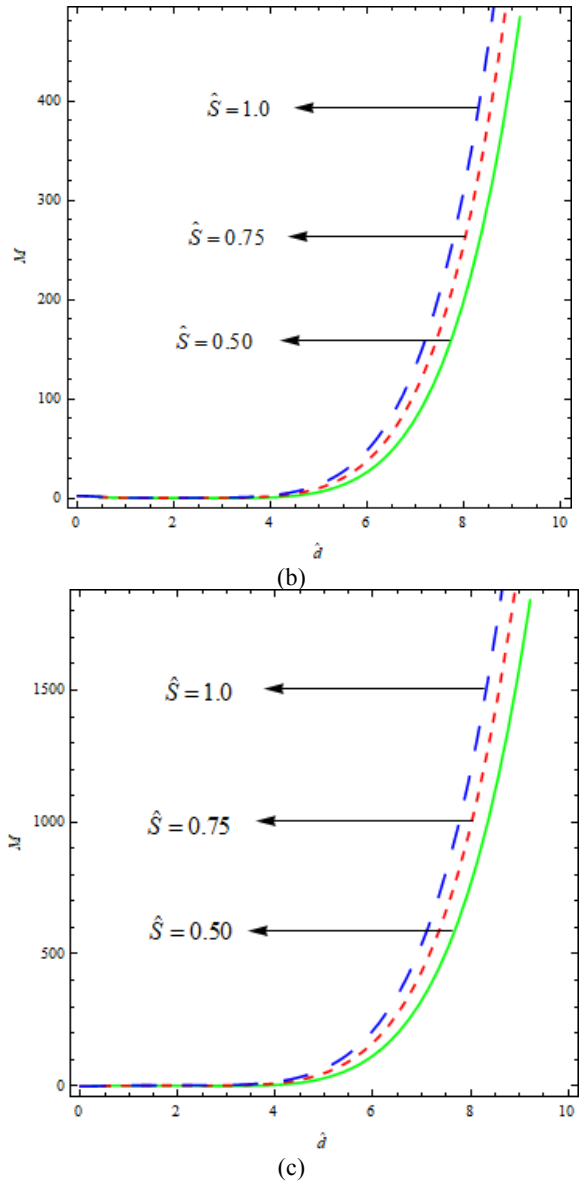

Fig. 5 M Versus $\hat{d}$ for different values of $\hat{S}$

The effect of solute diffusivity ratio $\hat{S}$ of the fluid, in fluid layer is depicted graphically in the Fig. 5(a, b, c) for the three profiles respectively. It is observed that the effect of $\hat{S}$ is to increase the thermal Marangoni numbers M_1, M_2 and M_3 irrespective of the temperature profiles. This suggests that $\hat{S}$ stabilizes the system.

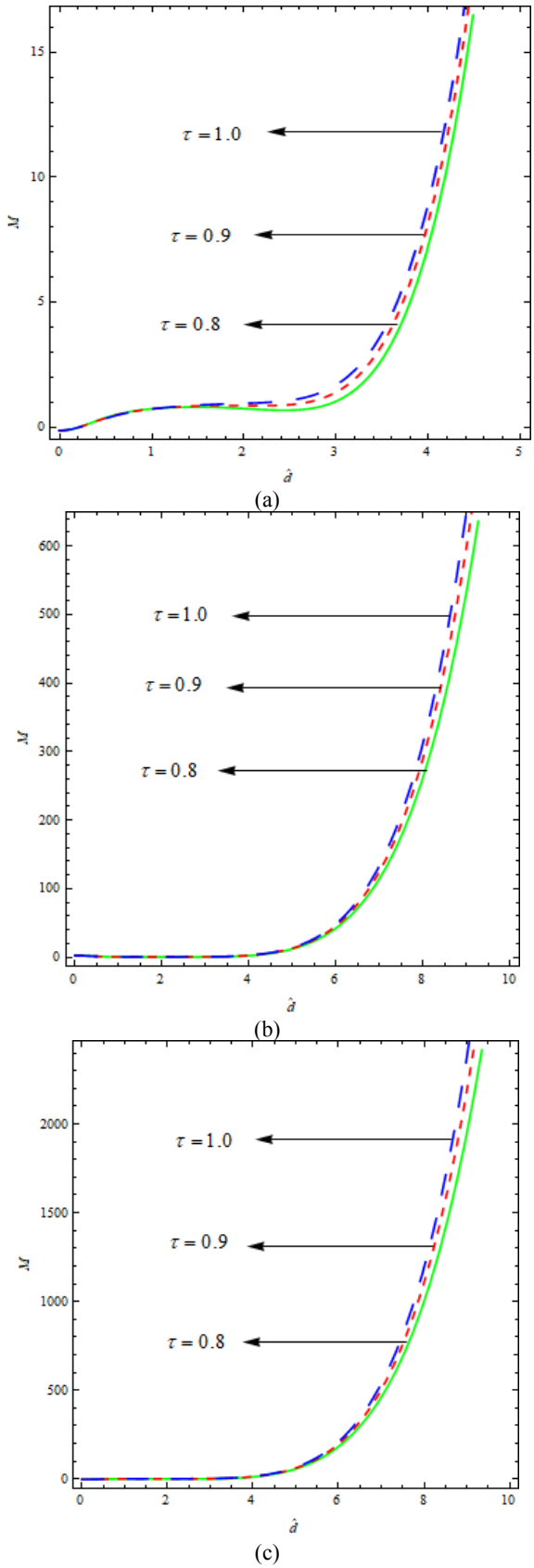

Fig. 6 M Versus $\hat{d}$ for different values of τ

Increase in the solute thermal diffusivity ratio τ of the fluid, in fluid layer, increases M_1, M_2 and M_3 for all the three temperature profiles which is shown in Fig. 6(a, b, c). Thus, the effect of τ is to stabilize the system.

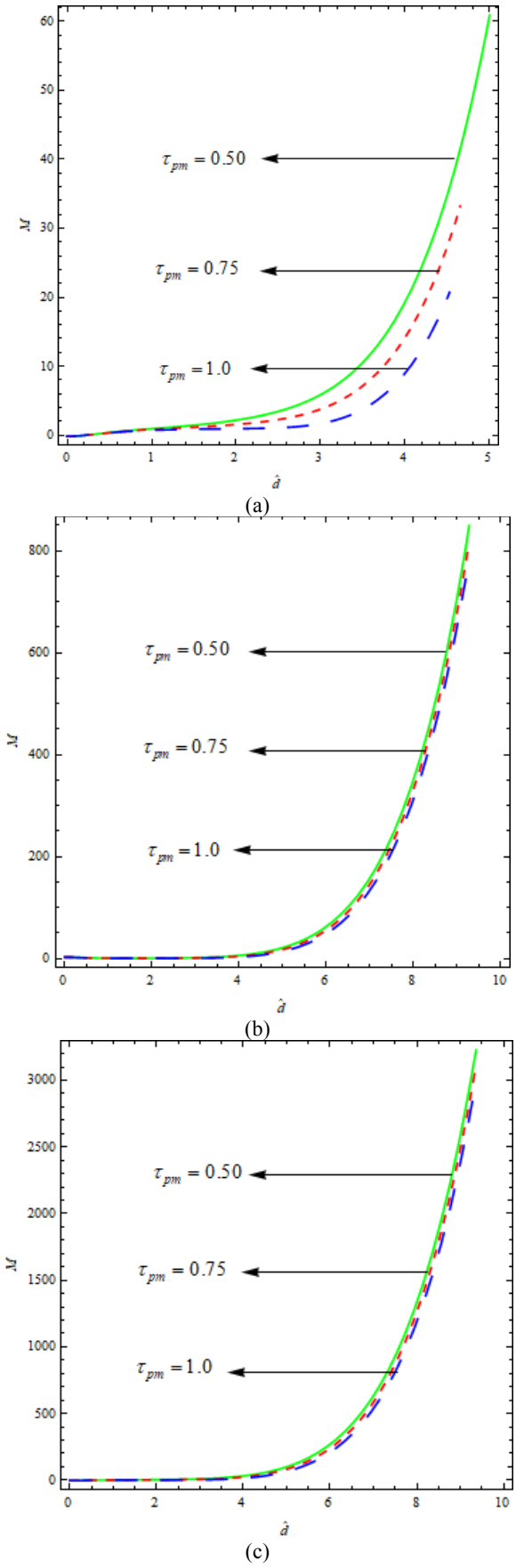

Fig. 7 M Versus $\hat{d}$ for different values of τ_{pm}

Fig. 7(a, b, c) depict the effect of solute thermal diffusivity ratio τ_{pm} of the fluid, in the porous region, on the thermal Marangoni numbers M_1, M_2 and M_3 for the three profiles, respectively. From the figures it is clear that the effect of τ_{pm} is to decrease the values of M_1, M_2 and M_3, this helps to quicken the onset of convection and hence the system is destabilized.

CONCLUSIONS

i. Inverted parabolic temperature profile can be utilized in the situations where convection needs to be augmented, parabolic for moderate convection and linear profile where the convection needs to be delayed.
ii. Thermal Marangoni number increases rapidly in the porous layer dominant composite layer.
iii. Solute and thermal diffusivity parameters can be effectively used to control the convection
iv. By adjusting the strength of the heat source, onset convection can be augmented or delayed.

ACKNOWLEDGEMENT

The author expresses his sincere thanks to the management of REVA University, Bengaluru for their encouragement and support.

REFERENCES

Akil J. Harfash., Fahad K. Nashmi., 2017. Triply resonant double diffusive convection in a fluid layer. *Mathematical Modelling and Analysis*, 22(6), 809-826.

Bennacer, R., Beji, H., Mohamad, A. A., 2003. Double diffusive convection in a vertical enclosure inserted with two saturated porous layers confining a fluid layer. *International Journal of Thermal Sciences*, 42(2), 141-151.

Chen C. F., Cho Lik Chan., 2010. Stability of buoyancy and surface tension driven convection in a horizontal double-diffusive fluid layer, *International Journal of Heat and Mass Transfer*, 53(7–8), 1563-1569.

Gangadharaiah, Y. H., Suma, S. P., 2013. Bernard-Marangoni convection in a fluid layer overlying a layer of an anisotropic porous layer with deformable free surface, *Advanced Porous Materials*, 1(2), 229-238.

Kanchana, C., YiZhao., P.G.Siddheshwar., 2020. Küppers–Lortz instability in rotating Rayleigh–Bénard convection bounded by rigid/free isothermal boundaries". *Applied Mathematics and Computation*, 385, 125406.

Massimo Corcione, Stefano Grignaffini, Alessandro Quintino, 2015. Correlations for the double-diffusive natural convection in square enclosures induced by opposite temperature and concentration gradients. *International Journal of Heat and Mass Transfer*, 81, 811-819.

Norazam Arbin, Nur Suhailayani Suhaimi, Ishak Hashim., 2016. Simulation on double-diffusive Marangoni convection with the presence of entropy generation. *Indian Journal of Science and Technology*, 9(31), DOI: 10.17485/ijst/2016/v9i31/97817.

Saleem, M., Hossain, M. A., Suvash C. Saha., 2014. Double diffusive Marangoni convection flow of electrically conducting fluid in a square cavity with chemical reaction. *J. Heat Transfer*, 136(6), 1-9.

Sheng Chen, Jonas Tlke, Manfred Krafczyk., 2014. Numerical investigation of double-diffusive (natural) convection in vertical annuluses with opposing temperature and concentration gradients. *International Journal of Heat and Fluid Flow*, 31(2), 217-226.

Sumithra, R., 2014. Double diffusive magneto Marangoni convection in a composite layer. *International Journal of Application or Innovation in Engineering & Management*. 3(2), 12-25.

Sumithra, R., Vanishree, R. K., Manjunatha, N., 2020. Effect of constant heat source / sink on single component Marangoni convection in a composite layer bounded by adiabatic boundaries in presence of uniform & non uniform temperature gradients. *Malaya Journal of Matematik*, 8(2), 306-313.

Tatyana Lyubimova., Ekaterina Kolchanova., 2018. The onset of double-diffusive convection in a superposed fluid and porous layer under high-frequency and small-amplitude vibrations. *Transport in Porous Media*, 122(11), 97-124.

Vanishree, R. K., Sumithra, R., Manjunatha, N., 2020. Effect on uniform and non uniform temperature gradients on Benard-Marangoni convection in a superposed fluid and porous layer in the presence of heat source". *Gedrag en Organisatie*. 33(2), 746-758.